

Organic Modifiers Promote Furfuryl Alcohol Ring Hydrogenation via Surface Hydrogen-Bonding Interactions

Patrick D. Coan, Carrie A. Farberow, Michael B. Griffin, and J. Will Medlin*



Cite This: *ACS Catal.* 2021, 11, 3730–3739



Read Online

ACCESS |



Metrics & More



Article Recommendations

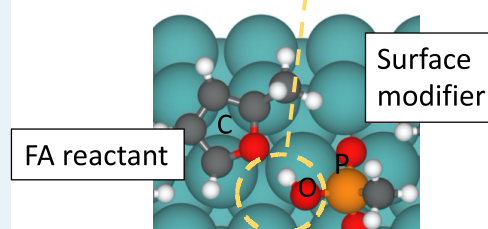


Supporting Information

ABSTRACT: Interactions between surface adsorbed species can affect catalyst reactivity, and thus, the ability to tune these interactions is of considerable importance. Deposition of organic modifiers provides one method of intentionally introducing controllable surface interactions onto catalyst surfaces. In this study, Pd/Al₂O₃ catalysts were modified with either thiol or phosphonic acid (PA) ligands and tested in the hydrogenation of furanic species. The thiol modifiers were found to inhibit ring hydrogenation (RH) activity, with the degree of inhibition trending with the thiol surface coverage. This suggests that thiols do not strongly interact with the reactants and simply serve to block active sites on the Pd surface. PAs, on the other hand, were found to enhance RH when furfuryl alcohol (FA) was used as the reactant. Density functional theory calculations suggested that this enhancement was due to hydrogen-bonding interactions between FA-derived surface intermediates and PA modifiers. Here, installation of hydrogen-bonding groups on the Pd surface served to preferentially stabilize RH product states. Furthermore, the promotional effect on the RH of FA was observed to be greater when a higher-coverage PA was used, providing a rate more than twice that of the unmodified Pd/Al₂O₃. The results of this work suggest that organic ligands can be designed to impart tunable surface interactions on heterogeneous catalysts, providing an additional method of controlling catalytic performance.

KEYWORDS: heterogeneous catalysis, catalyst modification, self-assembled monolayers, phosphonic acids, thiols, ring hydrogenation, furfuryl alcohol

H-bonding interactions promote hydrogenation



1. INTRODUCTION

Recent years have seen an increased focus on understanding the interactions between adsorbates in heterogeneous catalysis and how these interactions can be controlled to influence reactivity.^{1–6} In liquid-phase systems, for instance, it has been shown that the choice of solvent can significantly affect catalytic activity and selectivity via interactions with reactants, intermediates, or the catalyst surface.^{7–9} In some cases, particularly when water is used, the solvent can control surface reactivity by acting directly as a co-catalyst or aiding in the transport of reactants to active reaction sites.^{10–12} This approach has been further extended to gas-phase reactions, by taking advantage of water produced in situ or by co-feeding water into the system.^{1,9,13–15} Studies have also shown that interactions between reactants and/or intermediates present on the surface can promote activity. For example, surface oxygen atoms have been shown to assist in O–H bond activation on metals such as Pd¹⁶ and in C–H bond activation on Au catalysts.^{17,18}

One method for introducing highly controllable surface interactions is to intentionally load the catalyst with organic ligands, which can be chosen to exhibit desirable properties for a given reaction. For example, self-assembled monolayers (SAMs) deposited from various precursors, such as thiols or

amines, have been used to crowd the surface of metal catalyst particles in order to improve reactivity through steric and/or electronic effects.^{3,19,20} Additionally, it has been shown that modifiers can be specifically designed to take advantage of π – π interactions between an aromatic reactant and modifier, leading to significantly higher yield in the selective hydrogenation of cinnamaldehyde.²¹ More recent work has explored the use of phosphonic acids (PAs) as surface modifiers, which typically deposit onto metal oxide catalysts and supports.^{22–25} These studies have found that PA modifiers can enhance catalyst behavior by providing steric effects, improving catalyst stability, introducing additional active sites, or promoting the adsorption and subsequent reaction of an adsorbate.^{6,26–29} Moreover, organic PA modifiers have been shown to be surprisingly stable (to >300 °C) under high-temperature hydrogenation conditions.⁵ They are also stable under hydrothermal conditions, though oxidizing conditions are

Received: September 21, 2020

Revised: February 24, 2021

Published: March 9, 2021



known to degrade the organic ligands at temperatures near 200 °C.^{26,27}

In our previous work, we deposited PA modifiers onto Pd and Pt catalysts to improve the activity for hydrodeoxygenation (HDO) of aromatic oxygenates.^{30,31} Primarily, PAs were found to bind to the metal oxide support and enhanced HDO reactivity by providing Brønsted acid sites near the metal-support interface. When Pd was used as the catalyst, however, it was found that PAs were also deposited onto metal sites. Furthermore, this presence of PAs on the Pd surface was accompanied by a noticeable change in the activity for ring hydrogenation (RH) of furfuryl alcohol (FA) to tetrahydrofurfuryl alcohol (THFA).³⁰ In particular, the use of alkylphosphonic acids led to significantly enhanced RH activity, improving the apparent turnover frequency (TOF) by over an order of magnitude relative to the unmodified catalyst. Two hypotheses are proposed to account for how the RH activity might be improved by the presence of PA modifiers on the Pd surface: (1) selective site blocking by organic modifiers may discourage the accumulation of strongly adsorbed furanic species on Pd,³² thus leaving more active sites available for subsequent reactions; or (2) PAs may contribute to promoting the RH reaction via surface interactions, either by stabilizing a specific, favorable binding geometry or by participating directly in the reaction mechanism.

In this contribution, we focused on evaluating these hypotheses by studying the effects of organic surface modifiers on the RH of furanic species, using a combined experimental and computational approach. Pd/Al₂O₃ catalysts were modified with either thiol or PA ligands, the structures of which were varied to prepare catalysts having a comparatively high-coverage and low-coverage of each type of modifier, as outlined in Figure 1. The coverage of thiol modifiers on Pd has been previously shown to be controllable by selection of appropriate ligands. For example, use of adamantanethiol (AT)

produces a coverage near 2.4 nm⁻², whereas use of 1-octadecanethiol (C18SH) yields a coverage near 4.5 nm⁻².³³ Additionally, it has been shown in prior work that no thiol uptake occurs on bare Al₂O₃, indicating that these SAMs reside on the metal surface rather than the catalyst support.³⁴ Coverages of PAs on Pd have been estimated to be <2.2 nm⁻² and have also been shown to be controllable by steric bulk on Au/TiO₂.^{27,30} Unmodified and modified catalysts were then tested in the RH of furanic species containing a polar or nonpolar substituent, that is, FA and 2-methyl furan (2MF), shown in Figure 1. Here, we show that the use of thiol SAMs led to consistent and significant losses of RH activity, which trended with proportionate decreases in the active hydrogenation surface area. PA modifiers, however, were found to promote the RH activity when a polar substituent group was present on the furan ring despite a reduction in the number of active sites. These findings, along with the results of density functional theory (DFT) calculations, suggest that hydrogen-bonding interactions between PA modifiers and reactants can promote hydrogenation of the furanic ring to THFA, a raw material in the production of fine chemicals.^{35–40} While RH is used here as a model reaction, RH of oxygenated furanics is an important step in the upgrading of biomass.^{41–43} More broadly, the results presented here indicate that surface modifiers can be designed and employed to introduce desirable intermolecular surface interactions, providing an additional degree of freedom for directing catalyst activity.

2. EXPERIMENTAL METHODS

2.1. Materials and Sample Preparation. Pd/Al₂O₃ (1 wt %, ~3 nm particle size³⁴), 1-octadecanethiol (98%), 1-adamantanethiol (95%), *n*-butylphosphonic acid (*n*-BuPA) (98%), *t*-butylphosphonic acid (98%) (*t*-BuPA), FA (98%), 2MF (98%), 200 proof ethanol, and D₂ (99.6 at. % D) were purchased from Sigma-Aldrich. HPLC-grade tetrahydrofuran (THF) (>99.9%) was purchased from OmniSolv. Ultra-high purity H₂ and He were obtained from Airgas.

Thiol and PA modifiers were each deposited onto Pd/Al₂O₃ (1 wt %) by previously reported liquid deposition techniques.^{34,44} Thiolate SAMs were prepared by submerging 250 mg of Pd/Al₂O₃ into 40 mL of 5 mM thiolate/ethanol solution and allowing the mixture to settle for 12–16 h. The supernatant was then decanted, and 40 mL of fresh ethanol was added to rinse the catalyst of excess thiol. After 4 h, the supernatant was again decanted, and the catalyst was dried in air for 12 h before use. For the deposition of PAs, a 10 mM solution of PA in THF was prepared, containing at least a 3-fold excess of modifier predicted for a full monolayer (on the Al₂O₃ support). The desired mass of Pd/Al₂O₃ was then added to the solution, and the mixture was stirred for 12–16 h at ambient conditions. Next, the solid was separated by centrifugation using an Eppendorf 5804 centrifuge at 8000 rpm for 8 min and annealed at 120 °C for 6 h. The annealing step is needed for the condensation reaction that binds the phosphonate to metal oxide surfaces; note that this postdeposition annealing step was not used in the preparation of thiolate-coated samples. The catalyst was then washed three times in the same volume of THF used to prepare the initial deposition solution, to remove any excess PA. Finally, the modified catalyst was dried under vacuum at room temperature before use.

2.2. Catalyst Characterization. CO pulse chemisorption was performed using an Altamira Instruments AMI-300 system

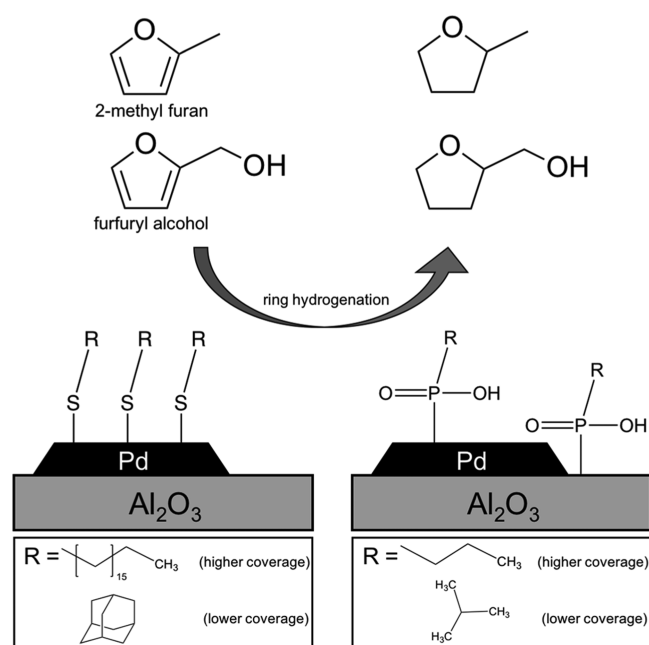


Figure 1. Proposed scheme showing the RH reactions studied, thiol deposition onto metals (left), and PA deposition onto both the metal and support (right). Tail structures used for each type of modifier, and the relative expected coverages, are shown below.

equipped with a thermal conductivity detector. Approximately, 50 mg of catalyst was loaded into a quartz U-tube reactor and held as a fixed bed on a plug of quartz wool. The sample was pretreated in 4% H₂/Ar flowing at 50 mL min⁻¹ by heating at 10 °C min⁻¹ to 180 °C and holding for 2 h. After the pretreatment, the sample was cooled to 30 °C and flushed with He flowing at 50 mL min⁻¹ for 10 min to remove any weakly adsorbed hydrogen. The sample was then exposed to sequential 500 μL pulses of a 10% CO/He gas mixture until saturation. A 500 μL sample loop was used to calibrate the TCD response. The surface area of the 1% Pd/Al₂O₃ catalyst was found to be approximately 49 ± 4 μmol/g, corresponding to a dispersion estimated at 53% ± 5%.

Diffuse reflectance infrared Fourier transform spectroscopy (DRIFTS) was performed on powder catalyst samples using a Thermo Scientific Nicolet 6700 FT-IR with a Harrick Scientific closed cell attachment. Spectra were collected in the hydrocarbon stretching region, using 100 scans and a resolution of 4 cm⁻¹, in order to confirm the identity of alkyl tails in the surface modifiers. Spectra of the unmodified Pd/Al₂O₃ catalyst were used as the background for all experiments so that the reported spectra of the modified catalysts represent only changes due to surface modification.

Hydrogen–deuterium exchange experiments were performed to measure the effect of each surface modifier on the catalytically active surface area for hydrogenation. Approximately 0.5 mg of catalyst, along with α-Al₂O₃ as a diluent, was loaded into a Pyrex tube, packed bed, continuous-flow reactor at atmospheric temperature and pressure. The effluent of the reactor was analyzed with a Pfeiffer Vacuum Prisma 80 quadrupole mass spectrometer. Samples were first purged in a 15 mL min⁻¹ Ar stream for 10 min, followed by a mixture of 15 mL min⁻¹ Ar and 5 mL min⁻¹ H₂ for at least 10 min. Next, while continuing to flow the Ar/H₂ mixture, three separate injections of 0.2 mL D₂ were slowly introduced to the feed stream and the resulting D₂ signals were measured. As a control, the same feed stream was then allowed to bypass the reactor, and three injections of 0.2 mL D₂ were again performed. The amount of D₂ detected in the reactor effluent with and without the presence of the catalyst was used to calculate the D₂ conversion, used as a measure of the H₂/D₂ exchange activity. Due to the large excess of H₂ relative to D₂ (~10:1 M ratio), the conversions measured in these pulse experiments are far from equilibrium. Data reported here were measured at conversions below 70%, while the use of larger catalyst masses allowed for conversions >95%, suggesting that the reverse reaction rate of H₂/D₂ scrambling was negligible. Experiments using only α-Al₂O₃ and no Pd catalyst did not yield any observable conversion of D₂.

2.3. Reactor Studies. Hydrogenation reactions were performed on FA and 2MF using a Pyrex tube, packed bed, continuous-flow reactor under atmospheric pressure. Helium was bubbled through the desired liquid reactant and held in a temperature-controlled bath (FA at 60 °C, 2MF at -10 °C), and the resulting stream was mixed with H₂ and make-up He upstream of the reactor. The reactor feed streams had a gas-phase mole fraction of Y_{H₂} = 0.10 and Y_{H₂} = 0.15 for reactions of FA and 2MF, respectively. All reactions were run using a 30:1 M ratio of H₂/reactant at a temperature of 180 °C. The mass of the catalyst used for each reaction was varied as needed (typically between 0.3 and 1.2 mg) to achieve a desired conversion. Due to the low mass of the catalyst required, both

the Pd/Al₂O₃ catalyst and an α-Al₂O₃ diluent were finely ground to a similar consistency prior to mixing, which was found to yield consistent results in repeated measurements with different catalyst beds. (Error bars for different catalyst beds are reported in the results). Both the feed streams and reactor effluents were analyzed using an SRI Instruments 8610C gas chromatograph equipped with a Restek MXT-5 capillary column and a flame ionization detector. Each reaction experiment was run to steady state, which was defined here as running for at least 150 min and having a conversion within ±0.5% over four consecutive measurements, taken over a period of 1 h. Final conversions of FA and 2MF were 5–15 and 15–30%, respectively, except for C18SH-modified catalysts which had conversions below 5% for both reactants. Average conversions and selectivities determined from the final steady state measurements were used to calculate the reported reaction rates.

2.4. DFT Calculations. Density functional theory calculations were performed using a plane-wave basis set as implemented in the Vienna ab initio simulation package.⁴⁵ The generalized gradient corrected PBE exchange–correlation functional⁴⁶ was used, and the ion–electron interactions were described using projector augmented-wave potentials⁴⁷ with an energy cutoff of 400 eV. Calculations were also performed using the optPBE-vdW functional to account for van der Waals interactions, and the corresponding energies are reported in enclosed square brackets following the PBE values.⁴⁸ The Pd(111) surface was modeled by a (3 × 3) unit cell, periodically repeated in a supercell geometry with successive four-layer slabs separated by 20 Å vacuum. The surface Brillouin zone was sampled using a 5 × 5 × 1 Monkhorst–Pack mesh. Surface adsorbates and atoms in the top two layers of the metal slab were allowed to relax whereas atoms in the bottom two layers were fixed in the bulk truncated positions. Optimizations were considered complete when forces fell below 0.05 eV/Å. The periodic Pd slab was modeled using an optimized lattice constant of *a* = 3.96 Å which closely matches the experimental value of 3.89 Å.⁴⁹ Binding energies (BE) reported on Pd(111) were calculated relative to the energy of the clean Pd(111) slab (*E*_{Pd(111)}) and the energy of the adsorbed species in the gas phase (*E*_{gas}).

$$BE = E_{\text{total}} - E_{\text{Pd(111)}} - E_{\text{gas}}$$

where *E*_{total} is the total energy of the slab with the adsorbed species. The differential BEs of FA and 2MF on the PA-modified Pd surfaces were calculated relative to the energy of the Pd(111) slab with the specified PA adsorbate (*E*_{PA/Pd(111)}) and the energy of the furanic species in the gas phase

$$\text{differential BE} = E_{\text{total}} - E_{\text{PA/Pd(111)}} - E_{\text{gas}}$$

where *E*_{total} is the total energy of the slab with FA or 2MF coadsorbed with the PA species.

3. RESULTS AND DISCUSSION

3.1. Catalyst Characterization. The uncoated Pd/Al₂O₃ (1 wt %) catalyst was modified with either one of two thiols or one of two PAs to probe the effect of the modifier head group on reactivity. The thiols, 1-octadecanethiol (C18SH) and 1-adamantanethiol (AT), were selected because they have been shown to form well-ordered SAMs with considerably different coverage on Pd catalysts.^{33,34,50,51} More specifically, the bulkier tail group present in AT results in a more sparsely packed

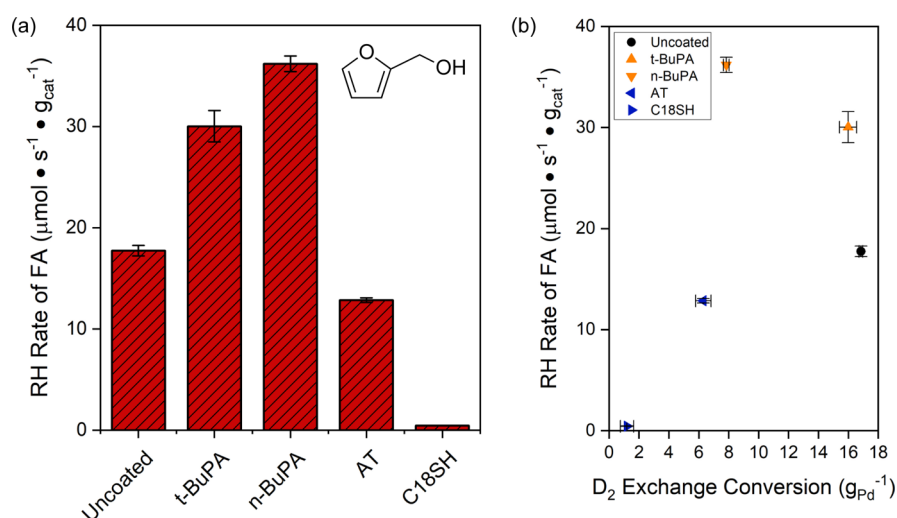


Figure 2. (a) Rates of RH of FA over uncoated and coated catalysts. $T = 180\text{ }^{\circ}\text{C}$, 30:1 M ratio of $\text{H}_2/\text{reactant}$, conversion = 5–15%. Error bars represent the standard deviation of triplicate measurements. (b) RH rates as a function of H_2/D_2 exchange activity.

monolayer with a nearest neighbor spacing of approximately 6.4 versus 4.7 Å for C18SH (or a density of ~ 2.4 vs $\sim 4.5\text{ nm}^{-2}$).³³ In a similar vein, *n*-BuPA and *t*-BuPA were chosen because the different tail structures are expected to result in different PA surface coverages.²⁷ Previous work using the more compact *n*-BuPA modifier indicated a nearest-neighbor spacing near 6.8 Å (~ 2 phosphonates- nm^{-2}), suggesting that the density of PA modifiers on Pd may be generally lower than that of thiols.³⁰ Still, in comparing the performance of each coated catalyst, the impact of both the modifier head group and relative coverage can be examined.

Catalysts modified with thiols and PAs were characterized by DRIFTS to confirm the presence and identity of modifiers on the surface (Figure S1). Spectra of the thiol-coated catalysts exhibited intense peak characteristics of C–H stretching modes that are consistent with previous studies.^{33,52} For both the C18SH and AT coatings, symmetric methylene stretching was observed near 2850 cm^{-1} . Asymmetric methylene stretching was observed on the C18SH-modified catalyst at 2920 cm^{-1} and on the AT-modified catalyst at 2918 cm^{-1} , indicating that both thiols formed ordered SAMs on Pd/ Al_2O_3 .^{25,51} Consistent with the respective tail structures, methyl stretching was detected in the C18SH coating (2954 cm^{-1}) but was not present after modifying with AT. Thus, the thiol modifiers maintain their tail structure during deposition onto Pd/ Al_2O_3 and form ordered, well-defined monolayers.

PA-modified catalysts were also characterized by clear C–H stretching peaks indicative of the modifier tail structure and in agreement with prior work.^{27,30,31} Both *n*-BuPA- and *t*-BuPA-modified catalysts exhibited methyl stretching peaks, with the symmetric mode observed in the range of 2870–2880 cm^{-1} . The asymmetric methyl stretching mode was observed at 2964 and 2956 cm^{-1} for *n*-BuPA and *t*-BuPA, respectively. In agreement with the modifier structures, methylene stretching was only detected after modification with *n*-BuPA, which exhibited an asymmetric methylene stretch at 2935 cm^{-1} . The relatively high frequency of this stretch indicates a fairly disordered monolayer, which is consistent with modifiers having short alkyl chains.^{25,27,30,51,52} Because the *t*-BuPA modifier does not contain methylene groups, the *t*-BuPA monolayer structure cannot be directly assessed in this way, though it is expected that monolayers formed by deposition of

n-BuPA and *t*-BuPA will be similarly disordered. This assumption is supported by previous reports that short-chain modifiers form more disordered monolayers.^{25,52} Finally, it is expected that PA modifiers bind to both the metal oxide support and the Pd surface, as has been shown in prior work from our laboratory.^{28,30} Overall, these results suggest that all modifier structures were preserved during deposition onto Pd/ Al_2O_3 , and while thiols formed highly ordered SAMs on the metal surface, PAs produced fairly disordered monolayers present on both the metal and support. Previous work using X-ray diffraction, nitrogen adsorption, and electron microscopy has demonstrated that deposition of these organic modifiers on Pd/ Al_2O_3 and similar materials has little influence on textural properties such as the phase of the Al_2O_3 catalyst support, the total surface area of the supported catalyst, or the average crystallite size, though in some cases the monolayers can stabilize nanomaterials exposed to harsh environments such as hydrothermal conditions.²⁶

The effect of each ligand on the hydrogenation-active surface area of the uncoated Pd/ Al_2O_3 catalyst was determined by measuring hydrogen-deuterium exchange rates, reported in Table S1. As anticipated, modification with C18SH strongly suppressed the availability of active sites for H_2/D_2 exchange, indicated by the $\sim 93\%$ decrease in the HD formation rate (Table S1). This result suggests a substantial surface coverage of C18SH, in agreement with previous reports on alkanethiol SAMs.⁵² AT, which has been reported to form less-dense SAMs due to its bulky tail, suppressed H_2/D_2 exchange rates to a lesser extent ($\sim 63\%$), consistent with a lower modifier coverage.^{50,51} Similar large changes in catalyst activity have been observed in studies of furfural decarbonylation (DC) chemistry when using C18SH and AT as surface modifiers.³⁴ Much like the thiol ligands, the two PA modifiers also had noticeably different effects on the rate of H_2/D_2 exchange, suggesting a difference in surface coverages. As predicted, the bulkier *t*-butyl tail suppressed H_2/D_2 exchange far less than PAs with *n*-butyl tails (5 and 54%, respectively), indicating a lower coverage of *t*-BuPA modifiers (Table S1). In general, a lower reduction in the H_2/D_2 exchange rates was observed after deposition of PAs relative to thiols. Specifically, the higher-coverage PA modifier reduced rates to a lesser extent than the lower-coverage thiol modifier (54% compared to

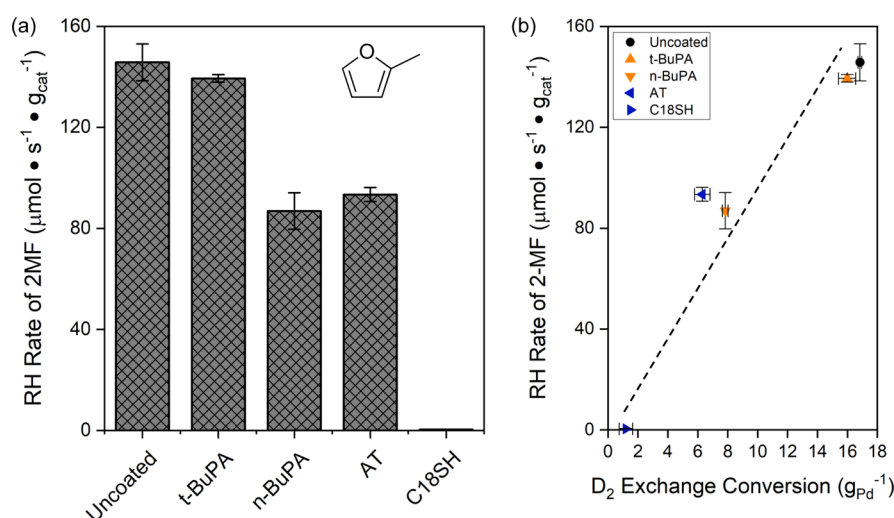


Figure 3. (a) Rates of RH of 2MF over uncoated and coated catalysts. $T = 180\text{ }^\circ\text{C}$, 30:1 M ratio of H_2 /reactant. (b) RH rates as a function of H_2 / D_2 exchange activity. Rates trend approximately linearly, indicated by the dotted line, suggesting the effect of modifiers on the RH of 2MF is due to site blocking. All error bars represent the standard deviation of triplicate measurements.

63%). This result is consistent with previously measured surface coverages discussed above, which indicated that the higher-coverage PA (*n*-BuPA) has a slightly lower density on Pd than even the sparse AT modifier (nearest-neighbor distance of ~ 6.8 to ~ 6.4 Å).^{30,33} The results of these experiments confirm that the bulkier modifiers (AT and *t*-BuPA) produce less-dense monolayers than ligands having the same binding group but straight alkyl tails (C18SH and *n*-BuPA) so that the effect of modifier coverage can be examined.

3.2. Hydrogenation Studies. Previous research from our group demonstrated that furan RH is accelerated by *n*-BuPA modifiers (and other alkyl PAs) on Pd/ Al_2O_3 catalysts.³⁰ This promotion of RH was found to originate from PA modifiers deposited on the Pd metal (and not the support) based on control experiments using PA-modified Pd black (where the PA significantly enhanced reaction rates) and physical mixtures of PA-modified Al_2O_3 and unmodified Pd/ Al_2O_3 (where no rate enhancement from the PAs was observed).³⁰ Here, we sought to determine whether other types of ligands could also promote this activity. Unmodified and modified Pd/ Al_2O_3 (1 wt %) catalysts were tested in the gas-phase hydrogenation of FA using a packed-bed, continuous flow reactor at $180\text{ }^\circ\text{C}$ and a steady state conversion of $<15\%$. The observed rates of RH are shown in Figure 2a, and sample time-on-stream data showing normalized conversions of each catalyst are reported in Figure S2a. In agreement with previously reported results, modification with *n*-BuPA was found to significantly enhance the RH activity, exhibiting a rate (per mass of Pd) more than twice that of unmodified Pd/ Al_2O_3 .³⁰ Additionally, the selectivity to the direct RH product, THFA, was found to be 87%, compared to 58% on the unmodified catalyst. Pd/ Al_2O_3 modified with *t*-BuPA, which blocks fewer Pd sites than *n*-BuPA based on the H_2 / D_2 exchange rates described above, exhibited a similar increase in the rate of RH and a THFA selectivity of 80%. However, the enhancement in RH was not as great as that observed with the *n*-BuPA modifier despite *n*-BuPA blocking a significantly greater number of sites. On the other hand, both of the thiol ligands suppressed the RH activity (Figure 2a) and had little effect on the THFA selectivity. The less-dense AT modifier reduced the RH rate by more than 25%, whereas C18SH nearly shut down the RH

pathway altogether, reducing the rate relative to the unmodified catalyst by $\sim 97\%$. The observed reductions in activity for the thiol-modified catalysts therefore appear to trend with the modifier coverages, as shown in Figure 2b. Previous work has reported similar effects of AT and C18SH modifiers on aromatic DC reactions.³⁴ Due to the preferred adsorption of aromatics in a flat-lying geometry at three-fold hollow sites, both DC and RH steps are proposed to occur over a contiguous ensemble of sites on metal terraces, and so site blocking by surface modifiers will similarly affect these two reactions.^{53–55} Pang et al. reported on the effects of thiol SAMs on reactions of furfural and found that AT modifiers reduced DC rates by nearly half, while C18SH modifiers reduced DC rates by $>99\%$.³⁴ Similarly, work by Lien et al. found that modification with AT and C18SH reduced the DC of benzyl alcohol by ~ 30 and 99%, respectively. Here, the comparable losses of H_2 / D_2 activity and RH rates on thiol modified catalysts (as shown in Figure 2b) further suggest that these modifiers mainly serve to block RH-active surface sites. We note that taking the ratio of the RH rate to the D_2 scrambling rate provides a rough measure of a relative TOF for different coatings. Based on the measured Pd dispersion of $\sim 53\%$, the TOF on the uncoated catalyst is approximately 0.3 s^{-1} . Using the D_2 scrambling rate as an indicator of surface area, we find that the apparent RH TOF is more than 4 times higher for the *n*-BuPA modified catalyst than the uncoated surface. If the CO chemisorption uptake is instead used to count available sites, the TOF would go up by an even larger factor of ~ 8 . This is because the CO uptake is suppressed by the PA coatings to an even greater extent than is D_2 scrambling, as shown in Table S1, though overall trends are similar.

Because modification with PAs promoted RH rates despite the coverage of hydrogenation sites, we hypothesized that the PAs provided a specific interaction which favored RH of FA. To explore the generality of these observed enhancements and the impact of the functional groups present in FA, we expanded the reaction testing to include the hydrogenation of 2MF. Reactions were performed under the same conditions as those used for FA, with the same ratio of H_2 /reactant, and at conversions of 15–30% (except for the C18SH-modified

catalyst which had conversions below 5%). Sample time-on-stream data showing the normalized conversions of each catalyst are reported in Figure S2b. In all experiments using 2MF, selectivity to 2-methyl tetrahydrofuran was observed to be >99%. As shown in Figure 3a, none of the surface ligands used in this study improved the RH performance of Pd/Al₂O₃ for 2MF. Modification with *t*-BuPA seemed to have little effect on the RH rate, in line with the relatively small suppression of H₂/D₂ exchange. The magnitude of RH rate suppression for *n*-BuPA and AT ligands was also consistent with H₂/D₂ exchange rates plotted in Figure 3b (i.e., 35–40% lower activity than the unmodified catalyst). Finally, C18SH again strongly limited the RH pathway, appearing to essentially eliminate the required active sites (Figure 3). Overall, the rates of hydrogenation of 2MF followed a similar trend to H₂/D₂ exchange rates, indicated by the apparent correlation in Figure 3b. However, the same trend was not observed for FA hydrogenation, particularly in the case of the PAs (Figure 2b). This analysis suggests that the effect of surface modifiers on the RH of 2MF is to simply block surface sites, resulting in a proportionate loss of RH activity. For the hydrogenation of FA, in contrast, it appears that specific interactions between the reactant and PA modifier permit this trend to be broken so that the presence of ligands on the surface actually enhances the RH rate.

3.3. DFT Calculations. DFT calculations were employed to examine how the PA head group affects the adsorption of each reactant, FA and 2MF. Because the structure of PAs adsorbed onto Pd and other metal surfaces is not well understood, the energetics associated with PA deposition were evaluated. The binding configuration for three different forms of adsorbed methylphosphonic acid (MPA), chosen as a simpler, model alkyl PA, was optimized on a Pd(111) surface at a density of 1.4 phosphonates-nm⁻². MPA was chosen as a model alkyl PA to probe local interactions between the head group and furanic reactants rather than to provide a highly precise simulation of the modified Pd surface. However, it is useful to note that MPA modifiers have been found to have similar promoting effects as *n*-BuPA for RH of FA on Pd/Al₂O₃. (The rate on MPA-modified Pd/Al₂O₃ was found to be ~10% higher compared to *n*-BuPA, perhaps due to a slightly higher coverage).³⁰ The configurations tested included molecular MPA, a dissociated phosphonate in which one O–H bond has been activated (MPA-1) and a doubly dissociated phosphonate in which both O–H bonds had been cleaved (methylphosphonate, MPA-2). Comparing the energy of these adsorbed states to MPA in the gas phase demonstrated that on Pd(111), the first O–H dissociation was thermodynamically favorable, whereas the second O–H dissociation to form MPA-2 was energetically uphill (Figure S3). For this reason, the following results focus on coadsorption of FA and 2MF with MPA-1, although details are provided for coadsorption of FA and 2MF with the MPA and MPA-2 adsorbates in the Supporting Information. Because the binding of PAs onto Pd and other metal surfaces is not well understood, the above additional results may provide insights for future studies.

The minimum energy optimized configuration for both FA and 2MF on Pd(111) at 1/9 monolayer (i.e., one adsorbate per nine surface Pd atoms) coverage, before and after PA modification, was found to be a flat-lying geometry nearly parallel to the Pd surface. The vertical distances between the Pd surface and the number two and four carbons of the furanic ring (Figure S4) are reported in Table S2; the corresponding

adsorption geometries are presented in Figure 4 (MPA-1) and Figure S5 (MPA, MPA-2). Energies reported below were

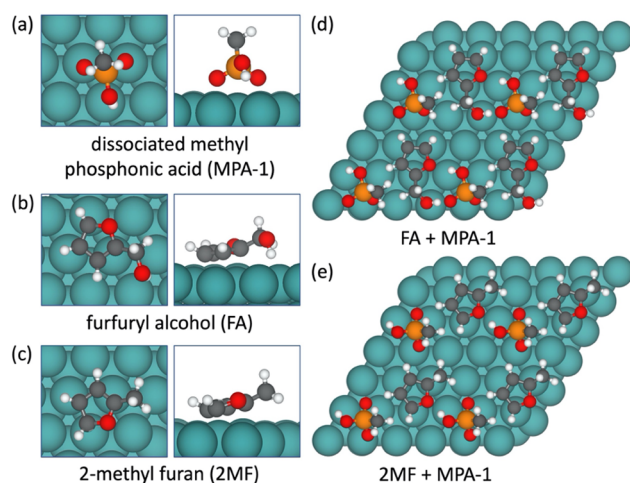


Figure 4. DFT calculated structures for the most stable molecular adsorption of (a) once-dissociated MPA, (b) FA on Pd(111), (c) 2MF on Pd(111), (d) FA on Pd(111) modified with MPA-1, (e) 2MF on Pd(111) modified with MPA-1. Color code: red = O, gray = C, white = H, orange = P, blue = Pd.

calculated both with and without van der Waals (vdW) interactions explicitly accounted for, as described in Section 2.4; the vdW calculations are indicated in brackets. On unmodified Pd(111), FA adsorption was 0.24 [0.30] eV more exothermic than 2MF adsorption as reported in Table 1, with each furanic reactant adsorbed in a similar flat-lying geometry (Figure 4b,c). On the MPA-1 coated surface, the adsorption of 2MF was destabilized by 0.29 [stabilized by 0.06] eV, whereas the adsorption of FA was stabilized by 0.08 [0.36] eV, making FA adsorption 0.61 [0.60] eV more exothermic than 2MF when coadsorbed with MPA-1 (Table 1). As shown in Figure 4, the adsorption of FA on the MPA-1 coated surface appears to be stabilized by hydrogen-bonding interactions between both the alcohol group and the furan ring oxygen and the PA head group. When no furanic reactant is present, the OH group in MPA-1 is pointed downward toward the Pd surface (Figure 4a). When MPA-1 is coadsorbed with 2MF or FA (Figure 4d,e), the OH group in MPA-1 tilts toward the oxygen in the furan ring, creating a hydrogen bond (O–H bond length of 1.74 and 1.92 Å for 2MF and FA, respectively). Additionally, when FA is coadsorbed with MPA-1, the alcohol group in FA is rotated with the oxygen atom oriented toward the Pd surface and the OH forming a comparatively shorter hydrogen bond with an oxygen in MPA-1 (O–H bond length 1.42 Å) that is likely stronger (Figure 4d). We note that in the coverage scenarios reported here, double-stabilization of FA by two hydrogen bond interactions had to occur with the O and OH of a single PA, although double stabilization of reactants by more than one co-adsorbed MPA-1 could occur when both functional groups are present. This may lead to an underestimation of the binding strength of FA in the presence of MPA-1 in this work. Overall, the stabilization of adsorbed FA compared to adsorbed 2MF on the PA-modified surface indicates a specific favorable interaction, which may play a role in the enhanced RH rates observed.

The MPA and less-stable MPA-2 modifier structures also showed stabilization of FA relative to 2MF (Table 1, Figure

Table 1. Differential BEs in eV (PBE [optPBE-vdW]) of FA and 2MF Adsorbed onto Unmodified Pd(111) and Pd(111) Modified with Various Forms of MPA

adsorbate	Pd(111)	Pd(111) + MPA	Pd(111) + MPA-1	Pd(111) + MPA-2
furfuryl alcohol	−1.00 [−1.66]	−1.26 [−2.10]	−1.08 [−2.02]	−1.15 [−2.17]
2-methyl furan	−0.76 [−1.36]	−0.85 [−1.62]	−0.47 [−1.42]	−0.70 [−1.65]
tetrahydrofurfuryl alcohol	−0.39 [−1.08]		−0.74 [−1.84]	

S5) as well as the reorientation of the alcohol group toward the PA modifier when compared to adsorbed FA on bare Pd(111). When MPA was used, both FA and 2MF were moderately stabilized compared to adsorption on the bare Pd(111) surface. For MPA-2, the modifier was found to slightly destabilize 2MF and stabilize FA when PBE energies are compared and stabilize both FA and 2MF when optPBE-vdW energies are compared, as with MPA-1. While there did not appear to be any specific interaction with 2MF, MPA-2 was a hydrogen-bond acceptor from FA.

4. DISCUSSION

Considering the combined experimental and computational results reported here, we surmise that the observed reactivity trends for thiol modifiers are primarily due to a loss of active surface area, whereas the trends for PA modifiers cannot be explained by simple site-blocking models. Although previous work using AT modifiers did lead to an increase in activity for benzyl alcohol deoxygenation, the higher rate was attributed to the prevention of carbonaceous species buildup, and surface DC reactions were still suppressed.⁵⁶ No such effects on RH due to modification with thiols were observed here. Furthermore, it has been shown that C18SH strongly reduces the accessibility of terrace sites on Pd nanoparticles, whereas both terrace and edge sites remain present after modification with AT.^{33,34} Thus, it is unlikely that the different effects of PA and thiol modifiers can be explained by the ligands possibly occupying different metal sites. It should be noted that the sulfur head group of the thiol modifiers is expected to have a more significant electronic influence on the Pd surface than PAs. However, even if electronic differences are significant, they do not appear to offer a clear explanation of why 2MF hydrogenation rates trend with D₂ exchange rates for all modifiers, but FA hydrogenation rates do not when PA modifiers are used.

Instead, the promotion of RH activity is likely related to our second hypothesis that a direct interaction with PA modifiers encourages the reaction of FA on Pd. The results of DFT calculations suggest that this specific interaction is related to hydrogen bonds formed between OH groups present on PA modifiers and both the alcohol functional group and furan ring oxygen in FA. This conclusion is consistent with the lack of RH promotion when 2MF was used as the reactant, as it lacks a polar functional group. Further support for this hypothesis comes from our previous work, which compared MPA and dimethylphosphinic acid (DMPA) surface modifiers.³⁰ DMPA is identical to MPA, except that one of the two OH groups on MPA is replaced by a methyl group. As our DFT calculations suggest that the most stable form of MPA on Pd has one OH group cleaved, it is expected that no OH group remains present on DMPA after deposition. When tested in the hydrogenation of FA, it was found that MPA modification improved RH to a similar degree as *n*-BuPA, while no improvement was observed after modification with DMPA. Thus, it appears that polar functional groups capable of

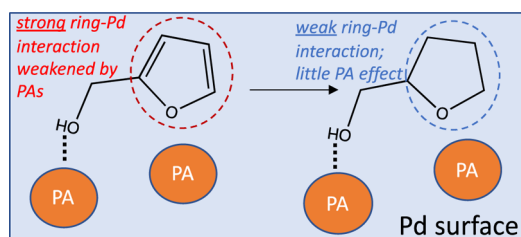
hydrogen bonding are required on both the modifier and reactant in order to produce enhanced activity.

In previous work, it was found that PAs promoted both HDO and RH reaction steps, and that the promotion of HDO required a protic O–H group on the modifier.³⁰ Here, it appears that the O–H group is also required for promotion of RH, serving to provide a unique surface interaction rather than introducing new acid sites. Another interesting observation is that while increasing the density of the thiol modifiers led to further suppression of RH activity, the more densely packed PA, *n*-BuPA provided a greater enhancement in the RH rate per mass of catalyst of FA than *t*-BuPA; the rate on the *n*-BuPA catalyst was roughly 20% higher. (In terms of apparent TOF, the rate enhancement associated with *n*-BuPA is even greater, nearly 80% higher, due to the fact that more sites are blocked). The higher rate after *n*-BuPA modification may be due to a higher likelihood of double-stabilization of FA by PAs on the Pd surface, as the results of DFT calculations indicated that PAs can interact with the alcohol group in FA as well as the oxygen in the furan ring. Although the promoting effect of PA modifiers appears to improve by increasing the ligand coverage, it is expected that at a sufficient coverage, the blocking of sites will outweigh the promoting effects; that is that there should exist an optimal modifier coverage. Note that determining the optimal modifier coverage is a complex task; here, we have assumed (based on prior work with other systems)²⁷ that PA coverage from *n*-BuPA modification is higher due to a low steric bulk of the alkyl tail group but the precise relationship between PA group sterics, coverage, and reaction rates is still not clear and warrants further study. Moreover, further study is needed to identify how additional substitution of the furyl ring (e.g., in 2,5-furandimethanol) affects the reaction system.

To further explore the hypothesis that H-bonding interactions can promote RH of FA, we calculated the overall surface reaction energy for the hydrogenation of adsorbed FA to form adsorbed THFA in the presence and absence of MPA-1 (i.e., FA* + 4H* → THFA* + 4*, where * indicates an adsorbed species or vacant Pd site). The strength of atomic hydrogen adsorption is essentially unaffected by the MPA-1 coadsorbate (BE = −0.60 [−0.45] eV and −0.61 [−0.49] eV on bare Pd(111) and on Pd(111) coadsorbed with MPA-1, respectively). On bare Pd(111), THFA adsorbs with a binding energy of −0.39 [−1.08] eV, giving a surface reaction energy of ΔE = 1.10 [0.65] eV. When coadsorbed with MPA-1, similar to FA, the hydrogen bonding interactions with MPA-1 at both the alcohol group and ring oxygen stabilize THFA (Figure S5, BE = −0.74 [−1.84] eV). The stabilization of THFA adsorption by MPA-1 is shown in Table 1. Moreover, in the case of the THFA, the stabilization due to MPA-1 is more significant, resulting in a more favorable overall surface reaction energy for hydrogenation (ΔE = 0.84 [0.42] eV). We propose that the relative stabilization of the product THFA is due to the weakening of the surface-ring interaction as the ring becomes saturated during the reaction. The H-bonding

interactions with the alcohol pendant group therefore become increasingly important in stabilizing the adsorbate (and, presumably, intermediate transition states). Moreover, the H-bonding stabilization appears to lead to adsorbed configurations in which the ring remains close to the active site: as seen in Table S2, adsorption of both FA and 2MF were more in-plane with the Pd surface when modified MPA-1. The results reported here then suggest that this “flatter” adsorption is correlated to enhanced RH rates. Scheme 1 provides a cartoon depiction showing how H-bonding interactions could lead to preferential stabilization of “product-like” species.

Scheme 1. Top View Schematic of Proposed Effects of PA Modifiers on Adsorption of “Reactant-like” and “Product-like” Intermediates^a



^aH-bonding with PA stabilizes adsorption of the FA reactant and THFA product but destabilizes the interaction between the Pd surface and the furan ring because more saturated rings interact with the Pd surface more weakly, this destabilizing effect on the Pd-furan ring interaction is lower in magnitude for the THFA product.

In considering ways to tune this type of promoting effect, one might expect that the electronic properties of the ligand would play a role and, in particular, that its acidity (or conjugate basicity) would be important. Previous work has shown that modification of Pd/Al₂O₃ and other supported metal catalysts with alkyl PAs creates Brønsted acid sites on the catalyst.^{6,30,31} In the prior work, temperature-programmed pyridine DRIFTS studies were used to show that the acidity of the catalyst could be tuned via changing the acidity of the PA precursor and that use of more acidic PAs improved activity for reactions such as HDO that are known to occur at the metal-support interface. However, most of the acidic sites monitored in those studies were associated with binding to the catalyst support rather than the metal. Preliminary studies of FA RH (which occurs on the metal) did not show that use of more acidic PAs (such as 2-phosphonoethanoic acid) improved RH rates.³⁰ Future work will investigate the possibility of using DFT calculations to design metal-bound PAs that form stronger H-bonds with furanic species, thus enabling stronger promotion of reactivity.

The combined experimental and computational results of this work suggest a valuable, relatively unexplored means of controlling the activity and selectivity of heterogeneous catalysts. Extensive work has been done on the use of modifiers to crowd surfaces or introduce catalytically active sites,^{6,30,31,57–59} though the approach of introducing and controlling surface interactions on solid metal catalysts has received less attention. One recent report, also focusing on the effects of hydrogen-bonding interactions, found that ligands containing hydrogen-bonding functionality significantly improved the selectivity and yield in the direct synthesis of hydrogen peroxide on Pd/C catalysts conducted in the liquid phase.⁶⁰ The work reported here suggests that these

phenomena may also be important in gas-phase reaction chemistries. Furthermore, the proposed H-bonding stabilization of particular surface intermediates or transition states can complement earlier methods that have focused on the use of monolayer tail groups for engineering specific interactions such as π - π stacking or acid-base interactions.^{21,28} In other words, both the binding/head group and the tail group of the ligands can be designed to tune catalytic performance. In fact, previous work with surface modifiers such as cinchonidine has indicated that hydrogen-bonding interactions between the modifiers and prochiral reactants can be the basis of enantioselective catalysis.^{61,62} While the ligands used here contained monofunctional tail groups, one could envision designing modifiers with multiple functional groups, further bridging the gap between highly active heterogeneous catalysts and the highly selective enzymes found in biological systems.

5. CONCLUSIONS

Pd/Al₂O₃ (1 wt %) catalysts were modified with different thiols and PAs to determine the effect of surface ligands on the RH of furanic species. Thiol SAMs were found to suppress the rate of RH for both FA and 2MF reactants, with the more densely packed C18SH ligand having a much stronger effect than the more sparsely packed AT. The degree of suppression was consistent with a reduction in active sites due to site-blocking by thiols, as indicated by the effect of these ligands on H₂/D₂ exchange rates. PA modifiers were found to enhance the rate of RH when FA was used as the reactant, with a higher PA coverage providing greater enhancement. DFT calculations showed that PAs formed hydrogen-bonding interactions with FA on the surface, preferentially stabilizing both FA and the hydrogenation product THFA compared to 2MF, based on the presence of a pendant OH group in FA. Overall, the results reported here show that PAs can be used to promote hydrogenation on Pd catalyst surfaces and that hydrogen-bonding interactions imparted by these modifiers can be used to control surface reactivity.

■ ASSOCIATED CONTENT

Supporting Information

The Supporting Information is available free of charge at <https://pubs.acs.org/doi/10.1021/acscatal.0c04138>.

Representative FT-IR spectra of Pd/Al₂O₃ after thiol or PA modification; complete RH and H₂/D₂ scrambling rates for unmodified and modified catalysts; energy profile for adsorption of MPA and its derivatives on Pd(111); DFT-calculated distances from Pd(111) to selected ring carbon atoms of adsorbed furanics; minimum energy adsorption geometries of FA and 2MF on Pd(111) surface modified with MPA and MPA-2; and minimum adsorption geometries of THFA adsorbed on Pd(111) and Pd(111) modified with MPA-1 (PDF)

■ AUTHOR INFORMATION

Corresponding Author

J. Will Medlin – Department of Chemical and Biological Engineering, University of Colorado-Boulder, Boulder, Colorado 80309, United States; orcid.org/0000-0003-2404-2443; Email: will.medlin@colorado.edu

Authors

Patrick D. Coan – Department of Chemical and Biological Engineering, University of Colorado-Boulder, Boulder, Colorado 80309, United States

Carrie A. Farberow – Catalytic Carbon Transformation & Scale-up Center, Golden, Colorado 80401, United States

Michael B. Griffin – Catalytic Carbon Transformation & Scale-up Center, Golden, Colorado 80401, United States

Complete contact information is available at:
<https://pubs.acs.org/10.1021/acscatal.0c04138>

Author Contributions

The manuscript was written through contributions of all authors. All authors have given approval to the final version of the manuscript.

Notes

The authors declare no competing financial interest.

ACKNOWLEDGMENTS

This work was supported by the Department of Energy, Office of Science, Basic Energy Sciences Program, Chemical Sciences, Geosciences, and Biosciences Division [grant no. DE-SC0005239]. This work was authored in part by the National Renewable Energy Laboratory, operated by Alliance for Sustainable Energy, LLC, for the U.S. Department of Energy (DOE) under Contract no. DE-AC36-08GO28308 with additional funding provided by the U.S. Department of Energy (DOE), Office of Energy Efficiency and Renewable Energy (EERE), Bioenergy Technologies Office (BETO), and in collaboration with the Chemical Catalysis for Bioenergy Consortium (ChemCatBio), a member of the Energy Materials Network (EMN). The views expressed in the article do not necessarily represent the views of the DOE or the U.S. Government. The U.S. Government retains and the publisher, by accepting the article for publication, acknowledges that the U.S. Government retains a nonexclusive, paid-up, irrevocable, worldwide license to publish or reproduce the published form of this work or allow others to do so, for U.S. Government purposes. A portion of the research was performed using computational resources sponsored by the Department of Energy's (DOE) Office of Energy Efficiency and Renewable Energy (EERE) and located at the National Renewable Energy Laboratory (NREL). P.D.C. also acknowledges partial support from the Department of Education Graduate Assistantship in Areas of National Need (GAANN).

REFERENCES

- (1) Saavedra, J.; Doan, H. A.; Pursell, C. J.; Grabow, L. C.; Chandler, B. D. The Critical Role of Water at the Gold-Titania Interface in Catalytic CO Oxidation. *Science* **2014**, *345*, 1599–1602.
- (2) Wu, B.; Huang, H.; Yang, J.; Zheng, N.; Fu, G. Selective Hydrogenation of α,β -Unsaturated Aldehydes Catalyzed by Amine-Capped Platinum-Cobalt Nanocrystals. *Angew. Chem., Int. Ed.* **2012**, *51*, 3440–3443.
- (3) Schrader, I.; Warneke, J.; Backenköhler, J.; Kunz, S. Functionalization of Platinum Nanoparticles with L-Proline: Simultaneous Enhancements of Catalytic Activity and Selectivity. *J. Am. Chem. Soc.* **2015**, *137*, 905–912.
- (4) Mallat, T.; Orglmeister, E.; Baiker, A. Asymmetric Catalysis at Chiral Metal Surfaces. *Chem. Rev.* **2007**, *107*, 4863–4890.
- (5) Schoenbaum, C. A.; Schwartz, D. K.; Medlin, J. W. Controlling the Surface Environment of Heterogeneous Catalysts Using Self-Assembled Monolayers. *Acc. Chem. Res.* **2014**, *47*, 1438–1445.
- (6) Zhang, J.; Ellis, L. D.; Wang, B.; Dzara, M. J.; Sievers, C.; Pylpyenko, S.; Nikolla, E.; Medlin, J. W. Control of Interfacial Acid-Metal Catalysis with Organic Monolayers. *Nat. Catal.* **2018**, *1*, 148–155.
- (7) Augustine, R. L.; Techaravapak, P. Heterogeneous Catalysis in Organic Synthesis. Part 9. Specific Site Solvent Effects in Catalytic Hydrogenations. *J. Mol. Catal.* **1994**, *87*, 95–105.
- (8) Mcmanus, I.; Daly, H.; Thompson, J. M.; Connor, E.; Hardacre, C.; Wilkinson, S. K.; Sedaie Bonab, N.; ten Dam, J.; Simmons, M. J. H.; Stitt, E. H.; et al. Effect of Solvent on the Hydrogenation of 4-Phenyl-2-Butanone over Pt Based Catalysts. *J. Catal.* **2015**, *330*, 344–353.
- (9) Li, G.; Wang, B.; Resasco, D. E. Water-Mediated Heterogeneously Catalyzed Reactions. *ACS Catal.* **2020**, *10*, 1294–1309.
- (10) Zope, B. N.; Hibbitts, D. D.; Neurock, M.; Davis, R. J. Reactivity of the Gold/Water Interface During Selective Oxidation Catalysis. *Science* **2010**, *330*, 74–78.
- (11) Zhao, Z.; Bababrik, R.; Xue, W.; Li, Y.; Briggs, N. M.; Nguyen, D.-T.; Nguyen, U.; Crossley, S. P.; Wang, S.; Wang, B.; et al. Solvent-Mediated Charge Separation Drives Alternative Hydrogenation Path of Furans in Liquid Water. *Nat. Catal.* **2019**, *2*, 431–436.
- (12) Janik, M. J.; Taylor, C. D.; Neurock, M. First-Principles Analysis of the Initial Electroreduction Steps of Oxygen over Pt (111). *J. Electrochem. Soc.* **2009**, *156*, B126–B135.
- (13) Hibbitts, D. D.; Loveless, B. T.; Neurock, M.; Iglesia, E. Mechanistic Role of Water on the Rate and Selectivity of Fischer-Tropsch Synthesis on Ruthenium Catalysts. *Angew. Chem., Int. Ed.* **2013**, *52*, 12273–12278.
- (14) Wang, C.; Gu, X.-K.; Yan, H.; Lin, Y.; Li, J.; Liu, D.; Li, W.-X.; Lu, J. Water-Mediated Mars–Van Krevelen Mechanism for CO Oxidation on Ceria-Supported Single-Atom Pt1 Catalyst. *ACS Catal.* **2017**, *7*, 887–891.
- (15) Nie, X.; Jiang, X.; Wang, H.; Luo, W.; Janik, M. J.; Chen, Y.; Guo, X.; Song, C. Mechanistic Understanding of Alloy Effect and Water Promotion for Pd-Cu Bimetallic Catalysts in CO₂ Hydrogenation to Methanol. *ACS Catal.* **2018**, *8*, 4873–4892.
- (16) Hibbitts, D. D.; Neurock, M. Influence of Oxygen and pH on the Selective Oxidation of Ethanol on Pd Catalysts. *J. Catal.* **2013**, *299*, 261–271.
- (17) Cremer, T.; Siler, C. G. F.; Rodríguez-Reyes, J. C. F.; Friend, C. M.; Madix, R. J. Tuning the Stability of Surface Intermediates Using Adsorbed Oxygen: Acetate on Au(111). *J. Phys. Chem. Lett.* **2014**, *5*, 1126–1130.
- (18) Xu, B.; Haubrich, J.; Baker, T. A.; Kaxiras, E.; Friend, C. M. Theoretical Study of O-Assisted Selective Coupling of Methanol on Au(111). *J. Phys. Chem. C* **2011**, *115*, 3703–3708.
- (19) Jia, X.; Ma, J.; Xia, F.; Xu, Y.; Gao, J.; Xu, J. Carboxylic Acid-Modified Metal Oxide Catalyst for Selectivity-Tunable Aerobic Ammoxidation. *Nat. Commun.* **2018**, *9*, 933.
- (20) Wu, B.; Huang, H.; Yang, J.; Zheng, N.; Fu, G. Selective Hydrogenation of α,β -Unsaturated Aldehydes Catalyzed by Amine-Capped Platinum-Cobalt Nanocrystals. *Angew. Chem., Int. Ed.* **2012**, *51*, 3440–3443.
- (21) Kahsar, K. R.; Schwartz, D. K.; Medlin, J. W. Control of Metal Catalyst Selectivity through Specific Non-Covalent Molecular Interactions. *J. Am. Chem. Soc.* **2014**, *136*, 520–526.
- (22) Nilsing, M.; Lunell, S.; Persson, P.; Ojamäe, L. Phosphonic Acid Adsorption at the TiO₂ Anatase (101) Surface Investigated by Periodic Hybrid HF-DFT Computations. *Surf. Sci.* **2005**, *582*, 49–60.
- (23) Lushtinetz, R.; Oliveira, A. F.; Duarte, H. A.; Seifert, G. Self-Assembled Monolayers of Alkylphosphonic Acids on Aluminum Oxide Surfaces—A Theoretical Study. *Z. Anorg. Allg. Chem.* **2010**, *636*, 1506–1512.
- (24) Bauer, T.; Schmaltz, T.; Lenz, T.; Halik, M.; Meyer, B.; Clark, T. Phosphonate- and Carboxylate-Based Self-Assembled Monolayers for Organic Devices: A Theoretical Study of Surface Binding on Aluminum Oxide with Experimental Support. *ACS Appl. Mater. Interfaces* **2013**, *5*, 6073–6080.

- (25) Ulman, A. Formation and Structure of Self-Assembled Monolayers. *Chem. Rev.* **1996**, *96*, 1533–1554.
- (26) Van Cleve, T.; Underhill, D.; Veiga Rodrigues, M.; Sievers, C.; Medlin, J. W. Enhanced Hydrothermal Stability of γ -Al₂O₃ Catalyst Supports with Alkyl Phosphonate Coatings. *Langmuir* **2018**, *34*, 3619–3625.
- (27) Jenkins, A. H.; Musgrave, C. B.; Medlin, J. W. Enhancing Au/TiO₂ Catalyst Thermostability and Coking Resistance with Alkyl Phosphonic-Acid Self-Assembled Monolayers. *ACS Appl. Mater. Interfaces* **2019**, *11*, 41289–41296.
- (28) Zhang, J.; Deo, S.; Janik, M. J.; Medlin, J. W. Control of Molecular Bonding Strength on Metal Catalysts with Organic Monolayers for CO₂ Reduction. *J. Am. Chem. Soc.* **2020**, *142*, 5184–5193.
- (29) Wang, C.; Hosomi, T.; Nagashima, K.; Takahashi, T.; Zhang, G.; Kanai, M.; Yoshida, H.; Yanagida, T. Phosphonic Acid Modified ZnO Nanowire Sensors: Directing Reaction Pathway of Volatile Carbonyl Compounds. *ACS Appl. Mater. Interfaces* **2020**, *12*, 44265–44272.
- (30) Coan, P. D.; Ellis, L. D.; Griffin, M. B.; Schwartz, D. K.; Medlin, J. W. Enhancing Cooperativity in Bifunctional Acid-Pd Catalysts with Carboxylic Acid-Functionalized Organic Monolayers. *J. Phys. Chem. C* **2018**, *122*, 6637–6647.
- (31) Coan, P. D.; Griffin, M. B.; Ciesielski, P. N.; Medlin, J. W. Phosphonic Acid Modifiers for Enhancing Selective Hydrodeoxygenation over Pt Catalysts: The Role of the Catalyst Support. *J. Catal.* **2019**, *372*, 311–320.
- (32) Kumar, G.; Lien, C.-H.; Janik, M. J.; Medlin, J. W. Catalyst Site Selection via Control over Noncovalent Interactions in Self-Assembled Monolayers. *ACS Catal.* **2016**, *6*, 5086–5094.
- (33) Schoenbaum, C. A.; Schwartz, D. K.; Medlin, J. W. Controlling Surface Crowding on a Pd Catalyst with Thiolate Self-Assembled Monolayers. *J. Catal.* **2013**, *303*, 92–99.
- (34) Pang, S. H.; Schoenbaum, C. A.; Schwartz, D. K.; Medlin, J. W. Directing Reaction Pathways by Catalyst Active-Site Selection Using Self-Assembled Monolayers. *Nat. Commun.* **2013**, *4*, 2448.
- (35) Chheda, J. N.; Huber, G. W.; Dumesic, J. A. Liquid-Phase Catalytic Processing of Biomass-Derived Oxygenated Hydrocarbons to Fuels and Chemicals. *Angew. Chem., Int. Ed.* **2007**, *46*, 7164–7183.
- (36) Song, Y.; Li, W.; Zhang, M.; Tao, K. Hydrogenation of Furfuryl Alcohol to Tetrahydrofurfuryl Alcohol on NiB/SiO₂ Amorphous Alloy Catalyst. *Front. Chem. Eng. China* **2007**, *1*, 151–154.
- (37) Chen, X.; Sun, W.; Xiao, N.; Yan, Y.; Liu, S. Experimental Study for Liquid Phase Selective Hydrogenation of Furfuryl Alcohol to Tetrahydrofurfuryl Alcohol on Supported Ni Catalysts. *Chem. Eng. J.* **2007**, *126*, 5–11.
- (38) Liu, S.; Amada, Y.; Tamura, M.; Nakagawa, Y.; Tomishige, K. One-Pot Selective Conversion of Furfural into 1,5-Pentanediol over a Pd-Added Ir-ReOx/SiO₂ Bifunctional Catalyst. *Green Chem.* **2014**, *16*, 617–626.
- (39) Chia, M.; Pagán-Torres, Y. J.; Hibbitts, D.; Tan, Q.; Pham, H. N.; Datye, A. K.; Neurock, M.; Davis, R. J.; Dumesic, J. A. Selective Hydrogenolysis of Polyols and Cyclic Ethers over Bifunctional Surface Sites on Rhodium-Rhenium Catalysts. *J. Am. Chem. Soc.* **2011**, *133*, 12675–12689.
- (40) Koso, S.; Ueda, N.; Shinmi, Y.; Okumura, K.; Kizuka, T.; Tomishige, K. Promoting Effect of Mo on the Hydrogenolysis of Tetrahydrofurfuryl Alcohol to 1,5-Pentanediol over Rh/SiO₂. *J. Catal.* **2009**, *267*, 89–92.
- (41) Serrano-Ruiz, J. C.; Dumesic, J. A. Catalytic Routes for the Conversion of Biomass into Liquid Hydrocarbon Transportation Fuels. *Energy Environ. Sci.* **2011**, *4*, 83.
- (42) Serrano-Ruiz, J. C.; Wang, D.; Dumesic, J. A. Catalytic Upgrading of Levulinic Acid to 5-Nonanone. *Green Chem.* **2010**, *12*, 574–577.
- (43) Chen, B.; Li, F.; Huang, Z.; Lu, T.; Yuan, Y.; Yuan, G. Integrated Catalytic Process to Directly Convert Furfural to Levulinic Ester with High Selectivity. *ChemSusChem* **2014**, *7*, 202–209.
- (44) Ellis, L. D.; Trottier, R. M.; Musgrave, C. B.; Schwartz, D. K.; Medlin, J. W. Controlling the Surface Reactivity of Titania via Electronic Tuning of Self-Assembled Monolayers. *ACS Catal.* **2017**, *7*, 8351–8357.
- (45) Kresse, G.; Furthmüller, J. Efficient Iterative Schemes for Ab Initio Total-Energy Calculations Using a Plane-Wave Basis Set. *Phys. Rev. B: Condens. Matter Mater. Phys.* **1996**, *54*, 11169–11186.
- (46) Perdew, J. P.; Burke, K.; Ernzerhof, M. Generalized Gradient Approximation Made Simple. *Phys. Rev. Lett.* **1996**, *77*, 3865–3868.
- (47) Kresse, G.; Joubert, D. From Ultrasoft Pseudopotentials to the Projector Augmented-Wave Method. *Phys. Rev. B: Condens. Matter Mater. Phys.* **1999**, *59*, 1758–1775.
- (48) Klimeš, J.; Bowler, D. R.; Michaelides, A. Chemical Accuracy for the van Der Waals Density Functional. *J. Phys.: Condens. Matter* **2009**, *22*, 22201.
- (49) ASM International. *ASM Handbook, Volume 3: Alloy Phase Diagrams*; ASM International: Materials Park, OH, 1992; pp 4–12.
- (50) Dameron, A. A.; Charles, L. F.; Weiss, P. S. Structures and Displacement of 1-Adamantanethiol Self-Assembled Monolayers on Au {111}. *J. Am. Chem. Soc.* **2005**, *127*, 8697–8704.
- (51) Love, J. C.; Wolfe, D. B.; Haasch, R.; Chabiny, M. L.; Paul, K. E.; Whitesides, G. M.; Nuzzo, R. G. Formation and Structure of Self-Assembled Monolayers of Alkanethiolates on Palladium. *J. Am. Chem. Soc.* **2003**, *125*, 2597–2609.
- (52) Chabiny, S. T.; O'Brien, M.; Oetter, B.; Corpuz, A.; Richards, R. M.; Schwartz, D. K.; Medlin, J. W. Controlled Selectivity for Palladium Catalysts Using Self-Assembled Monolayers. *Nat. Mater.* **2010**, *9*, 853–858.
- (53) Vorotnikov, V.; Mpourmpakis, G.; Vlachos, D. G. DFT Study of Furfural Conversion to Furan, Furfuryl Alcohol, and 2-Methylfuran on Pd(111). *ACS Catal.* **2012**, *2*, 2496–2504.
- (54) Bradley, M. K.; Robinson, J.; Woodruff, D. P. Surface Science The Structure and Bonding of Furan on Pd (111). *Surf. Sci.* **2010**, *604*, 920–925.
- (55) Pang, S. H.; Medlin, J. W. Adsorption and Reaction of Furfural and Furfuryl Alcohol on Pd(111): Unique Reaction Pathways for Multifunctional Reagents. *ACS Catal.* **2011**, *1*, 1272.
- (56) Lien, C.-H.; Medlin, J. W. Promotion of Activity and Selectivity by Alkanethiol Monolayers for Pd-Catalyzed Benzyl Alcohol Hydrodeoxygenation. *J. Phys. Chem. C* **2014**, *118*, 23783–23789.
- (57) Zeidan, R. K.; Hwang, S.-J.; Davis, M. E. Multifunctional Heterogeneous Catalysts: SBA-15-Containing Primary Amines and Sulfonic Acids. *Angew. Chem., Int. Ed.* **2006**, *45*, 6332–6335.
- (58) Zeidan, R.; Davis, M. E. The Effect of Acid–Base Pairing on Catalysis: An Efficient Acid–Base Functionalized Catalyst for Aldol Condensation. *J. Catal.* **2007**, *247*, 379–382.
- (59) Margelefsky, E. L.; Zeidan, R. K.; Davis, M. E. Cooperative Catalysis by Silica-Supported Organic Functional Groups. *Chem. Soc. Rev.* **2008**, *37*, 1118.
- (60) de L e Freitas, L. F.; Puértolas, B.; Zhang, J.; Wang, B.; Hoffman, A. S.; Bare, S. R.; Pérez-Ramírez, J.; Medlin, J. W.; Nikolla, E. Tunable Catalytic Performance of Palladium Nanoparticles for H₂O₂ Direct Synthesis via Surface-Bound Ligands. *ACS Catal.* **2020**, *10*, 5202–5207.
- (61) Borszky, K.; Bürgi, T.; Zhaohui, Z.; Mallat, T.; Baiker, A. Enantioselective Hydrogenation of α,β -Unsaturated Carboxylic Acids over Cinchonidine Modified Palladium: Nature of Modifier–Reactant Interaction. *J. Catal.* **1999**, *187*, 160–166.
- (62) Meheux, P.; Ibbotson, A.; Wells, P. B. Enantioselective Hydrogenation: II. Variation of Activity and Optical Yield with Experimental Variables in Methyl Pyruvate Hydrogenation Catalyzed by Cinchona-Modified Platinum/Silica (EUROPT-1). *J. Catal.* **1991**, *128*, 387–396.